AD A043275

BRL R 1996

BRL

AD

REPORT NO. 1996

PREDICTION OF SPIN-DECAY OF LIQUID-FILLED PROJECTILES

DDC
RECEIVED
AUG 25 1977
C

Clarence W. Kitchens, Jr.
Nathan Gerber

July 1977

Approved for public release; distribution unlimited.

USA ARMAMENT RESEARCH AND DEVELOPMENT COMMAND
USA BALLISTIC RESEARCH LABORATORY
ABERDEEN PROVING GROUND, MARYLAND

AD NO. _____
DDC FILE COPY

Destroy this report when it is no longer needed.
Do not return it to the originator.

Secondary distribution of this report by originating or sponsoring activity is prohibited.

Additional copies of this report may be obtained from the National Technical Information Service, U.S. Department of Commerce, Springfield, Virginia 22151.

The findings in this report are not to be construed as an official Department of the Army position, unless so designated by other authorized documents.

The use of trade names or manufacturers' names in this report does not constitute indorsement of any commercial product.

UNCLASSIFIED

SECURITY CLASSIFICATION OF THIS PAGE (When Data Entered)

REPORT DOCUMENTATION PAGE		READ INSTRUCTIONS BEFORE COMPLETING FORM
1. REPORT NUMBER BRL REPORT NO. 1996	2. GOVT ACCESSION NO. 14	3. RECIPIENT'S CATALOG NUMBER BRL-1996
4. TITLE (and Subtitle) Prediction of Spin-Decay of Liquid-Filled Projectiles		5. TYPE OF REPORT & PERIOD COVERED Final
		6. PERFORMING ORG. REPORT NUMBER
7. AUTHOR(s) Clarence W. Kitchens, Jr. Nathan Gerber		8. CONTRACT OR GRANT NUMBER(s) RDT&E 1W161102AH43
9. PERFORMING ORGANIZATION NAME AND ADDRESS USA Ballistic Research Laboratory Aberdeen Proving Ground, MD 21005		10. PROGRAM ELEMENT, PROJECT, TASK AREA & WORK UNIT NUMBERS 12 34
11. CONTROLLING OFFICE NAME AND ADDRESS US Army Materiel Development & Readiness Command 5001 Eisenhower Avenue Alexandria, VA 22333		12. REPORT DATE 11 JULY 1977 13. NUMBER OF PAGES 40
14. MONITORING AGENCY NAME & ADDRESS(if different from Controlling Office)		15. SECURITY CLASS. (of this report) UNCLASSIFIED 15a. DECLASSIFICATION/DOWNGRADING SCHEDULE

16. DISTRIBUTION STATEMENT (of this Report)

Approved for public release; distribution unlimited.

17. DISTRIBUTION STATEMENT (of the abstract entered in Block 20, if different from Report)

DDC
RECEIVED
AUG 25 1977
DISSEMINATED

18. SUPPLEMENTARY NOTES

19. KEY WORDS (Continue on reverse side if necessary and identify by block number)

Liquid-Filled Shell	Spin-Up	Flight Dynamics
Spin Decay	Navier-Stokes	Laminar
Finite-Difference	Boundary Layer	Turbulent
Wedemeyer Model	Unsteady Flow	Angular Momentum

20. ABSTRACT (Continue on reverse side if necessary and identify by block number)

An accurate method for predicting the spin-decay of liquid-filled projectiles throughout their flight is described. The method is based on Wedemeyer's model for the spin-up of the liquid payload. The in-bore spin-up process is predicted using numerical solutions of the Navier-Stokes equations and Wedemeyer's equation. Spin-decay calculations are compared to spin histories obtained from test firings of 155mm liquid-filled projectiles equipped with yawsondes. The 100%-filled cases show excellent agreement between the theory

DD FORM 1 JAN 73 1473 EDITION OF 1 NOV 65 IS OBSOLETE

UNCLASSIFIED

SECURITY CLASSIFICATION OF THIS PAGE (When Data Entered)

and the measurement throughout the entire flight; the errors being less than 0.8% of the measured spin rate. The errors are no larger than about 1% for 90%-filled cases. The theory is used to calculate the spin-up time of the liquid; defined as the time when 99% of the instantaneous rigid-body angular momentum is achieved.

TABLE OF CONTENTS

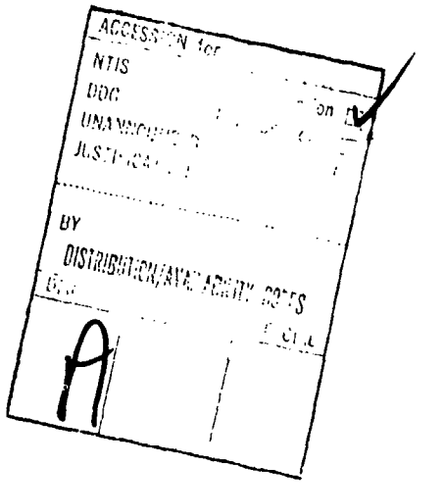

LIST OF ILLUSTRATIONS

PRECEDING PAGE BLANK-NOT FILMED

1. INTRODUCTION

The spin of all projectiles decreases along the flight path because of the aerodynamic torque arising from the skin friction on the exterior surface of the casing. The spin of a liquid-filled shell decreases more rapidly than one with a solid payload because angular momentum is transferred from the projectile casing to the liquid payload while the liquid is being spun up. Liquid spin-up is produced by the skin friction at the casing-liquid interface. We define the time in which the liquid, starting from zero spin, achieves a state of substantially solid-body rotation to be the spin-up period.

A study of the liquid motion during spin-up is important for several reasons. First, the frequencies of free oscillation of the liquid change during spin-up. These frequencies are needed to analyze the flight stability of a liquid-filled shell. Second, spin decay can decrease the gyroscopic stability factor of a liquid-filled shell to an unacceptable level. Third, the projectile spin-decay process may possibly lead to fluid dynamic instabilities in the liquid payload which could affect the shell motion. In this report only the spin-decay process is studied. The effect of spin decay on the frequencies will be reported separately.

The basis of the present work is a theory developed by Wedemeyer[1] which describes spin-up from rest of a liquid in a fully-filled cylindrical cavity. This theory accounts for a secondary flow, formed in the cavity as a result of the endwall boundary layers, which controls the spin-up process. Wedemeyer developed an equation for the azimuthal velocity during spin-up and solved for the velocity in closed form by neglecting viscous diffusion terms. He used this solution to derive approximate expressions for the rate of change of angular momentum of the liquid and calculate spin-decay of liquid-filled shell.

In this report we also calculate spin-decay, but our analysis differs from Wedemeyer's in several respects. First, we adopt Wedemeyer's azimuthal velocity equation describing the spin-up process, but retain the viscous diffusion terms he neglected. We determine the fluid angular momentum numerically from finite-difference solutions. Second, our analysis includes a technique for treating the non-impulsive spin-up process taking place in-bore the gun. This is used to determine the initial conditions for the subsequent spin-decay calculation in free flight. The accuracy of this technique is evaluated by comparing its results with those of finite-difference solutions of the Navier-Stokes equations; it is judged to be sufficient. Third, the aerodynamic spin damping effect is included in our analysis so the projectile spin can be accurately predicted throughout the entire flight.

---

1. *E. H. Wedemeyer, "The Unsteady Flow Within a Spinning Cylinder," J. Fluid Mech., Vol. 20, Part 3, 1964, pp. 383-399. Also see BRL Report 1252, Aberdeen Proving Ground, MD, October 1963. (AD 431846)*

PRECEDING PAGE BLANK-NOT FILMED

Spin-decay predictions obtained with these techniques are compared with measurements taken in test firings of the XM687 shell using a solar aspect sensor and telemetry technique[2]. The predicted spin decay is in excellent agreement with the measurements except for certain cases which show anomalous spin behavior; these cases are discussed in a separate report[3].

II. PROJECTILE SPIN-DECAY EQUATIONS

Consider a projectile containing a liquid-filled cylindrical cavity. Translational motion of the projectile in the gun imparts spin to it because of the barrel rifling. Spin-up of the liquid begins in-bore and continues after the projectile exits the gun tube. In free flight the spin rate of the casing, p, begins to decrease from its launch value, p_o, because of moments produced by two shear forces: 1) spin-decelerating moment due to air shear, M_{Aero}, and 2) liquid shear moment, M_{Liq}, which causes angular momentum to be transferred between the casing and the liquid payload. The projectile spin rate is determined from the equation of motion

$$I_z \, dp/dt = M_{Liq} + M_{Aero} \quad ; \tag{1}$$

where

$$M_{Aero} = \frac{\rho_a V^2}{2} S\ell C_{\ell_p} \left(\frac{p\ell}{V}\right) \quad , \tag{2}$$

$$M_{Liq} = - dL/dt \quad . \tag{3}$$

The quantity I_z is the axial moment of inertia of the empty projectile, V is the projectile velocity, S is the maximum projectile cross-sectional area, ℓ is the projectile diameter, ρ_a is the air density, C_{ℓ_p} is the projectile roll damping coefficient, and L is the liquid angular momentum. Since M_{Aero} is negative over the whole trajectory it causes p to

---

2. *A. Mark and W. H. Mermagen, "Measurement of Spin Decay and Instability of Liquid-Filled Projectiles Via Telemetry," BRL Memorandum Report 2333, Aberdeen Proving Ground, MD, October 1973. (AD 771919)*

3. *C. W. Kitchens, Jr., and R. Sedney, "Conjecture for Anomalous Spin Decay of the 155mm Binary Shell (XM687)," BRL Memorandum Report (in preparation).*

decrease. M_{Liq}, on the other hand, is negative at launch and in the early portion of the trajectory, but positive late in the flight. The liquid spin-up process, with $dL/dt > 0$, takes place during the in-bore and early free-flight phases. The moments acting on the casing during these phases are shown in Figures 1a, b. While the casing spin rate decreases, liquid spin-up proceeds until the liquid payload approaches a state of solid-body rotation. Solid-body rotation is never achieved because M_{Aero} continues to decrease the projectile spin rate. The liquid will eventually be "overspun" relative to the instantaneous projectile spin rate; that is, the local liquid angular velocity, $\omega = v/r$, will be greater than p, where v is the liquid azimuthal velocity and r is the radial coordinate. The liquid moment then reverses direction; i.e., $dL/dt < 0$, thus opposing the direction of the aerodynamic moment. This is illustrated in Figure 1c. During this phase the liquid acts to oppose further spin decay of the projectile.

We must know M_{Aero} and M_{Liq} as functions of p and t in order to be able to predict the spin rate from Eq. (1). The first is obtained from flight measurements using a projectile with a solid payload; M_{Liq} is determined by solving the equations of motion for the liquid. The boundary conditions for these equations involve the projectile spin rate which is the quantity we wish to determine. If the fluid motion is known, M_{Liq} can be found by integrating the shear stress acting on the sidewalls and endwalls of the cavity to obtain the resultant torque. An equivalent procedure, which is more convenient for the present purpose, uses Eq. (3). L(t) is defined by

$$L(t) = \rho \iiint r^2 v\ (r,z,t)\ d\theta dr dz \quad , \tag{4}$$

where the integral is taken over the cavity volume; r, θ, z are non-rotating cylindrical coordinates with z along the axis of the projectile, and ρ is the liquid density.

In our analysis we neglect the projectile yawing motion and assume that the spin-up flow is axisymmetric. Wedemeyer's spin-up theory[1] is used to determine v.

III. CALCULATION OF LIQUID ANGULAR MOMENTUM

A. The Wedemeyer Spin-Up Model

Wedemeyer[1] considered the problem of a circular cylinder filled with liquid which is initially at rest. At t = 0 it is given an impulsive angular velocity about its longitudinal axis and maintained at that value. He sought to determine the unsteady flow for all t, until the spin-up process ends with the fluid rotating uniformly as a rigid body.

The flow region is divided into two parts: (1) the thin Ekman boundary layers on the cylinder end walls; and (2) the remainder of the flow, called the core flow. He finds that the spin-up process is dominated by the Ekman layers. They create centrifugal pumping which causes secondary flow in the core. This flow enters the Ekman layers at $r(0 < r \leq r^*)$, is spun up, and then ejected back into the core at $r > r^*$, where r^* is the radial position of a shear layer propagating inward from the sidewall. This spinning fluid is then carried back into the interior of the cylinder. This mechanism of imparting rotation to the fluid is much more efficient than viscous diffusion alone.

Wedemeyer developed an approximate equation for the core flow through an order of magnitude analysis of the axisymmetric Navier-Stokes equations. In the core $v(r,z,t) \equiv v_c(r,t)$. The tangential momentum equation describing the core flow becomes

$$\partial v_c/\partial t + u_c(\partial v_c/\partial r + v_c/r) = \nu[\partial^2 v_c/\partial r^2 + \partial(v_c/r)/\partial r] \; ; \qquad (5)$$

where u_c and v_c are the radial and tangential velocity components in the core flow and ν is the liquid kinematic viscosity. The analysis shows that u_c and the axial velocity w_c, the secondary flow referred to above, are small compared to v_c, but not negligible, and that u_c and v_c are independent of z. The pressure P_c is given by

$$\partial P_c/\partial r = \rho v_c^2/r \quad . \qquad (6)$$

Conservation of mass relates u_c to the outward radial mass flow in the Ekman layers. An assumption is then made for the relation between the Ekman layer mass flow and v_c by interpolating between the known results for $t \to 0$ and $t \to \infty$.

Wedemeyer obtains two relationships for u_c depending on whether the endwall boundary layers are expected to be laminar or turbulent:

$$u_c = -0.443\ (a/c)Re^{-\frac{1}{2}}\ (rp-v_c) \quad , \quad \text{for } Re < 3\times10^5 \qquad (7)$$

and

$$u_c = -0.035\ (a/c)Re^{-1/5}\ (rp-v_c)^{8/5}/(ap)^{3/5} \quad , \text{ for } Re > 3\times10^5 \; ; \qquad (8)$$

where c is the cavity half-height, a is the cavity radius, and the Reynolds number is

$$Re = p\ a^2/\nu \quad . \qquad (9)$$

In his formulation of the spin-up problem he assumes p is constant, but in his application of this to spin decay p is a function of time. We shall also take p to be a function of time, both in free flight and in-bore the gun. A discussion and justification of the latter situation is given in Section III.C.

The initial and boundary conditions for Eq. (5) are

$$v_c(r,t) = 0 \quad \text{for } t < 0,$$
$$v_c(0,t) = 0 \quad \text{and} \quad v_c(a,t) = ap \quad \text{for } t \geq 0 \quad . \tag{10}$$

During projectile in-bore travel p(t) is specified using the spin history calculated from an interior ballistics trajectory. In free flight p(t) cannot be independently specified; it must be calculated from Eq. (1) including both the aerodynamic and liquid moments.

The total angular momentum of the liquid within the cylinder can be expressed using Eq. (4) with v equal to v_c, yielding

$$L = 4\pi c\rho \int_0^a r^2 v_c dr \quad . \tag{11}$$

B. Computation Procedures

The authors have employed two procedures using Eq. (1) to calculate spin-decay of liquid-filled shell. Method I is based on a numerical solution of Eq. (5); Method II is based on Wedemeyer's approximate expressions for rate of change of angular momentum. A third method, Method III, uses a Navier-Stokes calculation to predict in-bore liquid spin-up.

In Method I calculations are performed by simultaneously solving Eqs. (1), (5) and (11), using (2) and (3). Eq. (5) is solved by a second-order accurate finite-difference technique described by Sedney and Gerber[4]. In Method I we rewrite Eq. (1) as

$$I_z dp/dt = -dL/dt + p\, f(t) \quad ; \tag{12}$$

where

$$f(t) = \rho_a V S \ell^2 C_{\ell_p}/2 \tag{13}$$

is a known function of time depending on the projectile shape, velocity and the trajectory. We assume that all variables are known at time

4. *R. Sedney and N. Gerber, "Viscous Effects in the Wedemeyer Model of Spin-Up from Rest," BRL Report (in preparation).*

t_n, either through initial conditions or subsequent calculations and we wish to determine p and L at time t_{n+1}. We can express Eq. (12) by a second-order accurate finite-difference representation

$$I_z(p_{n+1}-p_n)/\Delta t = -(L_{n+1}-L_n)/\Delta t + [p_{n+1}f(t_{n+1}) + p_n f(t_n)]/2 \quad (14)$$

and solve for p_{n+1}, to obtain

$$p_{n+1} = \frac{p_n[I_z + \Delta t\ f(t_n)/2] - L_{n+1} + L_n}{[I_z - \Delta t\ f(t_{n+1})/2]} . \quad (15)$$

Eq. (15) relates the spin and angular momentum at t_{n+1} with $f(t_n)$, $f(t_{n+1})$, p_n, L_n, Δt and I_z prescribed.

The fluid angular momentum L_{n+1} must be calculated from Eqs. (5) and (11) using the sidewall boundary condition $v_c(a,t_{n+1}) = ap(t_{n+1})$. These equations give us a second relationship between p_{n+1} and L_{n+1} which is very complicated. This is combined with Eq. (15) to provide two equations for p_{n+1} and L_{n+1} which are solved numerically. We adopt an iteration procedure on L_{n+1} to retain second-order accuracy in the solution. The procedure employed is to guess L^1_{n+1} using linear extrapolation based on values at previous times and solve Eq. (15) for p_{n+1}. Eq. (5) is then solved using p_{n+1} as a boundary condition to yield $v_c(r,t_{n+1})$. The angular momentum L^2_{n+1} is calculated and compared with the guessed value L^1_{n+1}. If they differ by more than a set tolerance, ϵ, the calculation is repeated using L^2_{n+1} as the guess in Eq. (15). This iteration process is repeated until the desired tolerance is achieved. A value of $\epsilon = L_o \times 10^{-5}$ was used in all calculations described in this report and convergence was achieved in one to three iterations. This procedure can treat either laminar or turbulent endwall boundary layers through the specification of Eq. (7) or Eq. (8) for u_c in Eq. (5).

Method II is a simpler procedure, based on an ordinary differential equation for angular momentum which is solved simultaneously with Eq. (12). Equations for both laminar and turbulent cases were derived by Wedemeyer[1], assuming that Eq. (5) is valid for non-constant spin rate. In the laminar case, Eqs. (5) and (7) are combined and integrated in r to form an equation for the time rate of change of liquid angular momentum. This equation contains a viscous term representing the moment due to the shear stress along the sidewall. Wedemeyer approximated the

shear stress using an analytical "inviscid" solution obtained by neglecting the viscous terms on the right-hand side of Eq. (5). This approximation is not valid late in free flight when the liquid is overspun relative to the shell, because it does not account for the reversal of the liquid moment. Wedemeyer's equation for angular momentum in the laminar case is

$$dL/dt = -.886\,(a/c)(Re_o)^{-\frac{1}{2}}(p/p_o)^{\frac{1}{2}}\,(Lp_o - L_o p) - 8(Re_o)^{-1}\,pL_o\,[1 - L_o p/(Lp_o)] \tag{16}$$

where

$$L_o = \pi\rho c p_o a^4 \qquad \text{and} \qquad Re_o = p_o a^2/\nu \quad . \tag{17}$$

L_o is the reference angular momentum for a fluid in solid-body rotation with $v_c = p_o r$, p_o is the instantaneous shell spin rate when it exits the gun muzzle and Re_o is the launch Reynolds number.

For the turbulent case, Wedemeyer used the same procedure with Eqs. (5) and (8) and also approximated the sidewall shear stress using the "inviscid" solution for the laminar case. An additional assumption was required to evaluate an integral which depended on the shape of the velocity profile; he assumed the velocity profile could be approximated by the inviscid, laminar solution. Under these assumptions the expression for the turbulent case becomes

$$dL/dt = 0.035\,(a/c)(Re_o)^{-1/5}\,(p_o L_o)(p/p_o)^{9/5}\,[1-Lp_o/(L_o p)]^{8/5} \times [Lp_o/L_o p)]^{-13/5}\,4\int_0^{Lp_o/L_o p} X^{8/5}\,(1-X)^{-3/10}\,dX - 8(Re_o)^{-1}\,pL_o\,[1 - L_o p/(Lp_o)] \quad . \tag{18}$$

The terms on the right-hand side of Eqs. (16) and (18) represent the moments acting on the fluid due to the shear stress at the sidewall and endwalls. The first group of terms in each equation, containing $Re_o^{-\frac{1}{2}}$ and $Re_o^{-1/5}$, respectively, represent the moment due to the endwalls. The terms containing Re_o^{-1} represent the moment due to the sidewall. The sum of these two moments equals the time rate of change of angular momentum of the liquid.

To calculate the shell spin decay in the second procedure, Eq. (16) or Eq. (18) is solved simultaneously with Eq. (12). Although simpler than Method I, Method II has the drawback that the approximations involved in evaluating the shear stress at the sidewall (and describing $v_c(r,t)$ in the turbulent case) are not accurate during the late free-flight phase, Fig. 1c, where $dL/dt < 0$. We have, however, used both procedures and compared their predictions against the measured spin decay of liquid-filled XM687 shell.

C. In-Bore Spin-Up Effects

The first step in calculating projectile spin decay is to determine the amount of angular momentum achieved by the liquid during the in-bore spin-up process. This prescribes the initial conditions for the subsequent spin-decay calculation. Karpov[5] carried out experiments with 20mm M56 shell to study the spin-decay process and instability during spin-up. He presented spin histories for firings in a vacuum by correcting for spin deceleration due to the aerodynamic moment. He found that higher viscosity liquids reach "constant spin" sooner and at a level considerably different from that predicted by conservation of angular momentum. He thus was able to infer the percentage of the reference angular momentum L_o that was acquired while the projectile was still in the gun. L_o, Eq. (17), the maximum angular momentum that can be achieved by the liquid is never attained in actual firings because of the short time in the barrel and the spin-decay of the casing. For a 70%-filled case with $Re_o = 6500$ he found that 24% of L_o was achieved in-bore. For higher Reynolds number cases the percentage was smaller; e.g., with $Re_o = 6.5\times10^6$ the angular momentum at muzzle exit was 10% of L_o. While these actual percentages will not apply to other shell or gun tubes, they illustrate that significant liquid spin-up can occur in-bore the gun.

Wedemeyer[1] neglected the in-bore spin-up process in predicting spin decay; the angular momentum calculations began as the shell exited the gun. Also, Wedemeyer's equation, Eq. (5), is based on the assumption of impulsive spin-up from rest. The spin-up process actually begins in-bore from a non-impulsive start. As the shell accelerates the rotation rate increases, reaching p_o at muzzle exit. By the time the shell reaches the muzzle the liquid may have a significant portion of L_o, especially for smaller Re_o. Since part of the liquid is already rotating by the time that the projectile reaches the muzzle exit, the spin

5. *B. G. Karpov, "Dynamics of Liquid-Filled Shell: Instability During Spin-Up," BRL Memorandum Report 1629, Aberdeen Proving Ground, MD, January 1965. (AD 463926)*

decelerating effect on the casing is less than would be predicted by assuming an impulsive start at the time the shell exits the gun.

In order to treat in-bore spin-up, we assume that Wedemeyer's equation based on impulsive spin-up, Eq. (5), can be used in cases where the spin acceleration is very large. For a typical shell the spin acceleration is more than 4,800 rev/s^2, making it almost impulsive. We have compared the predicted in-bore angular momentum history from Method I with results from a numerical solution of the Navier-Stokes equations.

In our work the in-bore shell motion is predicted using an interior ballistics trajectory computer program, and this history is used together with the gun twist to determine the casing spin rate boundary condition. Figure 2 shows an example of a typical in-bore spin history for an XM687 shell launched at charge three from the M109 howitzer using M3 propellant. The variable t* is time measured from the beginning of projectile in-bore motion. The spin rate increases as the shell accelerates down the tube, exiting 19 ms after firing with a spin rate p_o = 92.3 rev/s, corresponding to a muzzle velocity V_o = 284.7 m/s.

The angular momentum acquired by the liquid during in-bore spin-up depends on the in-bore spin history, the cavity dimensions and the fluid properties. In Method I the in-bore angular momentum history is calculated using Wedemeyer's model by specifying the shell spin history during in-bore travel. Figure 3 shows predictions for the in-bore angular momentum history for two modified XM687 shell. Round 7670 contains a highly viscous oil ($\nu = 5\times10^{-4}$ m^2/s) with Re_o = 3320; the laminar endwall boundary-layer assumption, Eq. (7)is used. This calculation predicts that the liquid angular momentum is 18.6% of L_o at shell exit. Round 7675 contains water ($\nu = 1\times10^{-6}$ m^2/s) and has a much higher launch Reynolds number ($Re_o = 1.7\times10^6$); therefore, the turbulent endwall boundary layer assumption, Eq. (8), is used. The water payload thus spins up much slower than the oil acquiring only 2.6% of L_o at muzzle exit.

In Method III a finite-difference procedure is used to solve the Navier-Stokes equations. The flow is assumed axisymmetric, with u, v, w and P functions of r, z and t. This formulation does not require an endwall compatibility condition, such as Eq. (7). The entire flow is calculated without separating the problem into boundary layer and core regions. Analytical transformations of r and z permit grid points to be densely grouped near the endwalls and sidewall to aid in resolving the boundary layers. A numerical solution is obtained for equations describing vorticity and circulation using a modification of the predictor-corrector multiple iteration method of Rubin and Lin[6]. The stream

---

6. *S. G. Rubin and T. C. Lin, "A Numerical Method for Three-Dimensional Viscous Flow: Application to the Hypersonic Leading Edge," J. Comp. Phys., Vol. 9, 1972, pp. 339-364.*

function equation is solved by successive line relaxation. A separate report[7] will give details of the Navier-Stokes procedure and compare results from it with those from Wedemeyer's model.

Results from the Navier-Stokes equations for the in-bore angular momentum history are shown by the dashed curve in Figure 3 for Round 7670. This calculation used a 21×41, r-z grid and took 22 time steps to reach muzzle spin conditions, requiring 5.2 minutes of CPU time on the UNIVAC 1108. Longer computing times would be required for larger Reynolds numbers. Method III predicts an angular momentum level that is 2.5% larger at muzzle exit than that predicted by Method I. The discrepancy between these two calculations remains almost constant after about 6 ms. A Navier-Stokes calculation has not been made for Round 7675 because of the large Reynolds number and the expected turbulent flow in the endwall boundary layer. On the basis of the comparisons for Round 7670, we feel justified in using Method I for the in-bore angular momentum history of the liquid.

IV. COMPARISON WITH MEASURED SPIN DECAY

Spin decay predictions have been made for XM687 shell launched from the M109 howitzer and compared with measurements obtained using a solar aspect sensor and telemetry technique[2]. The motion of the projectile is determined by the use of photovoltaic cells which sense the orientation of the shell relative to the sun. The measuring system, called a yawsonde, is carried on-board the projectile and data are transmitted to a ground station through an FM/FM telemetry link. Data are not acquired during the in-bore spin-up process, but are first received shortly after the shell exits from the gun tube. The data reduction procedure yields both the yawing motion of the projectile and the spin history over the whole trajectory.

The standard XM687 contains two liquid-filled cylindrical canisters separated by discs which rupture on launch, producing a single cylindrical cavity. Data which can be compared directly with the present theory were obtained by Mark[8] at Wallops Island, VA, in May 1975 using a nonstandard cavity in the XM687 shell. The two-canister configuration was replaced with a single cylindrical cavity having a height of 0.474 m and a diameter of 0.107 m. These dimensions are approximately the dimensions of the cylindrical cavity in the standard XM687 after rupture of the discs. Shell filled with oil and with water were fired to give two quite different launch Reynolds numbers, approximately 3.3×10^3 and

---

7. *C. W. Kitchens, Jr., "Navier-Stokes Solutions for Spin-Up from Rest in a Cylindrical Container," BRL Report (in preparation).*

8. *A. Mark, "Measurement of Angular Momentum Transfer in Liquid-Filled Shell," BRL Report (in preparation).*

1.7×10^6, respectively. The standard XM687 is approximately 90% filled, and in these special firings fill ratios of both 90 and 100% were used. Table I provides a summary of the firing data for the five rounds for which comparisons are presented between the yawsonde measurements and the predicted spin decay. Round 10G2, containing a dual canister, was fired at Nicolet, Canada, during the 1974-75 winter tests[9] under different meteorological conditions than the other rounds. For all calculations discussed in this report the spin damping coefficient was described by

$$C_{\ell_p} = 0.00860\ M - 0.0200 \qquad \text{for} \qquad 0.53 \leq M \leq 0.84 \ , \qquad (19)$$

where M is the instantaneous free flight Mach number. Eq. (19) was determined from firings of XM687 containing solid filler as discussed in Reference 8. The air density and temperature needed to define the spin damping function, Eq. (13), were determined from meteorological data and the projectile velocity was deduced from radar measurements. The spin damping functions for two representative cases are shown in Figure 4. Round 10G2 was fired at 65° quadrant elevation with high air density. Round 7675 was fired at 30° quadrant elevation with almost standard density. All rounds exhibit the concave-downward shape shown in Figure 4. The spin damping functions for Rounds 7670, 7676 and 7677 are almost identical to that for Round 7675.

A. Fully-Filled Shell

The predicted spin-decay for round 7670 is compared with the yawsonde measurement in Figure 5. This round was filled with oil ($\nu = 5\times10^{-4}$ m^2/s); the firing data for this and subsequent rounds are shown in Table I. The total time of flight was 28s; only the first ten seconds are shown in Figure 5 because the spin-up process is completed by this time. The spin-decay history deduced from the yawsonde measurement is shown by the solid curve. Data acquisition began 0.1s after launch and the measured data were smoothly extrapolated back to a calculated value of spin at the muzzle. For each round the spin at the muzzle was calculated using the known gun tube twist and the independently measured muzzle velocity.

In the theoretical results shown in Figure 5 (note the broken ordinate scale) the endwall boundary-layers were assumed to be laminar. Assuming an impulsive start, calculations were made using Method I (shown by filled circles) and Method II (shown by filled triangles). The results from these two calculations are almost identical. The

---

9. *V. Oskay and J. H. Whiteside, "Flight Behavior of 155mm (XM687 Mod I and XM687 Mod II) and 8-Inch (XM736 Mod I) Binary Shell at Nicolet, Canada, During the Winter of 1974-1975," BRL Memorandum Report 2608, Aberdeen Proving Ground, MD, March 1976. (AD B010566L)*

Table I. Firing Data for XM687 Shell

Round No.	7670	7675	7676	7677	10G2
Fluid Payload	Oil	Water	Water	Oil	Freon 113/ Ethyl Alcohol
% Fill	100	100	90	90	89
Type Cavity	Single Cylinder	Single Cylinder	Single Cylinder	Single Cylinder	Dual Canister
Re_o	3.32×10^3	1.69×10^6	1.70×10^6	3.42×10^3	7.81×10^5
M_o	0.83	0.84	0.85	0.85	0.90
V_o (m/s)	284.7	289.8	291.8	293.4	281.3
Quadrant Elevation (degrees)	30	30	30	30	65
Beginning of Yawsonde Data (s)	0.10	2.50	0.19	0.07	0.10
End of Yawsonde Data (s)	26.6	23.9	28.5	28.0	46.9

calculated spin decay rate, assuming an impulsive start, is larger than the observed decay rate. This is due to the neglect of the in-bore spin-up process. At t = 10s the difference is 0.4%.

When in-bore effects are included in Method I, the results (shown by open circles in Figure 5) agree better with the measurement. The in-bore spin-up process described in Section III. C was used for the 19ms prior to t = 0. Time zero is defined to be the time when the projectile clears the gun tube. The predicted spin-up process was completed at t = 1.4s; for t > 1.4s the shell is in the late free-flight phase, shown in Figure 1c, wherein the direction of the liquid moment reverses. At this time the predicted spin rate, including in-bore effects, was 0.13% larger than the measured value. Calculations including in-bore effects have not been made for Method II. The predicted and measured spin-decay curves cross each other at 18s and the predicted spin rate is 0.43% lower than the measured value when the yawsonde data end at 26.6s. This cross-over can probably be traced to inaccuracies in the measured C_{ℓ_p} which causes the spin damping term f(t) to be too large.

When the launch Reynolds number is greater than 3×10^5 the endwall boundary layers are expected to be at least partially turbulent. The measured spin decay for round 7675, filled with water, is compared with results from the present theory with turbulent Ekman layers in Figure 6. Methods I and II both predict a more rapid spin decay than is observed experimentally; Method I gives the better agreement. At this large Reynolds number in-bore effects are not significant and both calculations with Method I (filled and open circles) give similar results. The predicted time of reversal of the liquid moment is 24.5s. At this time the predicted spin rate is 0.79% lower than the measurement, as extrapolated from the available yawsonde data which ends at 23.9s.

B. Partially-Filled Shell

At the present time a spin-up model for the partially-filled case does not exist, and the treatment of many cases of interest is hampered by the lack of such a theory, since most liquid-filled shell are only partially-filled. It would be useful to learn if the methods developed here for the filled cylinder could be used with any confidence for predicting spin decay in partially-filled cylinders. We might expect this if the fill ratio, β, is not much less than 90%.

The presence of the free surface in the partially-filled case introduces many complexities to the spin-up flow during in-bore acceleration and launch. This complex motion is discussed in Reference 10.

---

10. Engineering Design Handbook, Liquid-Filled Projectile Design, AMC Pamphlet No. 706-165, U.S. Army Materiel Command, Washington, DC, April 1969, p. 8-4. (AD 853719)

Briefly, the liquid moves rearward in the cavity under the action of in-bore accelerating forces and then forward due to air drag as the shell enters free flight. The process whereby the free surface forms near the rear endwall of the cavity as the shell emerges from the gun tube may vary considerably, depending on the actual fill ratio of the cavity. This liquid motion in-bore and during the early part of the flight possibly aids in mixing the rotating fluid near the cavity sidewall with the non-rotating fluid away from the wall. The importance of this effect on the spin decay history of partially-filled shell is not presently known.

The Wedemeyer spin-up theory has been applied to partially-filled XM687 shell, treating the shell as though it were fully-filled. The spin history of two XM687 (again having a single cylindrical cavity) with $\beta = 0.90$ are compared with predictions using this theory. Comparisons for Round 7677 (Table I) are shown in Figure 7. The spin history for this laminar, 90%-filled case is almost identical to that observed for the fully-filled case shown in Figure 5. Methods I and II both give reasonable agreement with the measured spin decay. Method I, including in-bore effects, is slightly more accurate; at 10s it predicts a spin rate that is 0.18% larger than the yawsonde measurement, whereas Method II predicts a value that is 0.29% smaller.

Similar comparisons for a much higher Reynolds number are shown in Figure 8 for round 7676 which is 90%-filled with water. It is assumed that the endwall boundary layers are turbulent in this case. The spin history is qualitatively different than that observed for the 100%-filled case in Figure 6. The most noticeable difference occurs in the first few seconds of the flight; the 90%-filled case loses spin much faster than the 100%-filled case. In the first half-second of flight the 90%-filled case loses 2.0% of its muzzle spin rate, whereas the 100%-filled case only loses 1.2%. This is surprising because it seems to indicate that the spin-up process in the 90%-filled case with a turbulent endwall boundary layer is faster than in the 100%-filled case. This may possibly be due to the mixing caused by the liquid shifting from the rear to the front of the cavity as the round emerges from the gun tube. Definite conclusions about this cannot be reached because β is not the only parameter that varies in these two firings.

Figure 8 shows that for $\beta = 1.00$ and turbulent Ekman layers, the theory predicts a more gradual spin decay in the first few seconds of the flight than is observed for the $\beta = 0.90$ round. Method I gives a more accurate prediction of the shell spin decay than Method II. At 10s Method II predicts a spin rate which is in error by approximately 1% while Method I essentially matches the experimental measurement. Since this shell with $\beta = 0.90$ doesn't appear to have the same spin decay history as the 100%-filled shell one should be cautious in attempting to apply Wedemeyer's fully-filled spin-up theory to this case.

V. DISCUSSION OF FLUID SPIN-UP TIME

Solid-body rotation is never completely achieved in a liquid-filled projectile because p is constantly changing. This is illustrated in Figure 9 which shows liquid azimuthal velocity profiles predicted with Method I at three instants in the flight of round 7675. The azimuthal velocity normalized by ap_o at the sidewall, r/a = 1.0, decreases with time. A typical velocity profile for solid-body rotation is shown for t = 27.5s by the dashed straight line $v_c = rp$. This state is not achieved at any time during this flight; at t = 27.5s $v_c < rp$ for $0 < r/a < 0.57$ and $v_c > rp$ for $0.57 \leq r/a < 1$. The fluid in the latter range of r is "overspun" relative to the projectile at this time; i.e., the local fluid angular velocity, $\omega_c = v_c/r$, is greater than p. Shortly after the liquid near the sidewall becomes overspun M_{Liq} reverses direction, opposing M_{Aero}. The spin-up process is then in the late free-flight phase shown in Figure 1c.

At a given time, solid-body rotation is more closely approached for small Re_o, because diffusion effects are greater. This is illustrated in Figure 10 which shows $v_c/(ap_o)$ predicted for round 7670. The approach to solid-body rotation for round 7670 is much more rapid than for round 7675, primarily due to the much lower Reynolds number. Also, the liquid in round 7670 approaches solid-body rotation much more closely. As an example, at t = 27.5s the largest difference between the predicted azimuthal velocity and solid-body rotation is less than 0.30%; for round 7675 differences of 4% for r/a = 0.90 and -18% for r/a = 0.20 are obtained.

It would be convenient to have a unique definition of spin-up time, but this is not possible because of the asymptotic approach to solid-body rotation. Also, depending on the application, different measures of the approach to solid-body rotation are appropriate. A comparable situation exists in defining the thickness of a boundary layer. Since this report is concerned with spin decay, we adopt a definition which uses the calculations of Method I. A separate report will discuss other definitions.

The spin-up time, t_s, is the time, measured from t = 0, at which the fluid angular momentum reaches 99% of the rigid-body angular momentum, when the latter is based on the instantaneous shell spin rate p. Figure 11 shows angular momentum, L, for rounds 7670 and 7675 as predicted by Method I, including in-bore effects. L is normalized by L_r, the angular momentum the fluid would have if it were rotating as a rigid-body at the instantaneous shell spin rate. As t increases $L/L_r \rightarrow 1$; it can exceed unity late in the flight when the fluid is in

the overspun state. This can occur even if $v_c < rp$ for fluid at small r because the overspun fluid at large r gives the dominant contribution to the integral for L, Eq. (11). Late in the flight $L/L_r > 1$ for both rounds in Figure 11, but it is only obvious for round 7675 because of the small scale of the plot. Normalizing L with the constant L_o would be convenient, but then L/L_o is non-monotonic and has a maximum that is always less than one. According to our definition of spin-up time, we obtain $t_s = 0.9$s for round 7670 and $t_s = 19.0$s for round 7675. The large difference in values of t_s results from the factor of 10^3 difference in Reynolds number.

It should be pointed out that the angular momentum predictions shown in Figure 11 do not agree with the results shown in Figure 13 of Reference 2, wherein the instantaneous liquid angular momentum is calculated by fitting measured yawsonde spin rate data and numerically integrating the projectile roll equation. For a typical XM687, round E1-5977 with $Re_o = 1.7\times10^6$, it is concluded in Reference 2 that only 85% of the instantaneous rigid-body angular momentum is achieved in the 30s time of flight. The present calculations predict that 85% of L_r is achieved in approximately 0.7s for round 7675 with $Re_o = 1.7\times10^6$. The large difference between these results for spin-up time appears to be caused by the inaccurate value for C_{ℓ_p} used in Reference 2 and the neglect of in-bore effects[8]. More recent calculations of angular momentum transfer[8] show better agreement with the present results.

VI. CONCLUSIONS

This report has described two methods based on Wedemeyer's spin-up theory[1] for predicting the spin-decay of liquid-filled projectiles throughout their flight. Shell spin histories are predicted by coupling the solution of the axial spin decay equation for the projectile to the solution for the liquid spin-up process.

Method II, based on an ordinary differential equation for liquid angular momentum, is strictly applicable only during the spin-up process. It does not apply late in the flight when the liquid is "overspun" relative to the shell spin rate; i.e., the shear stress acting on the casing reverses direction and M_{Liq} opposes further shell spin decay. This effect is accounted for in Method I, based on a numerical solution of Wedemeyer's spin-up equation, Eq. (5). Here the diffusion term is retained in Wedemeyer's equation and finite-difference solutions are obtained for the spin-up process. Method I gives better agreement with experimental measurements for shell spin decay than Method II.

The liquid angular momentum in-bore has been calculated using numerical solutions of the Navier-Stokes equations and Wedemeyer's equation. The results show that in some XM687 firings, with high viscosity oil, approximately 19% of the liquid rigid-body angular momentum is attained in-bore in less thar one revolution of the shell. The inclusion of in-bore spin-up in the spin decay calculations with Method I improved the agreement with the experimental measurements, significantly more so for small Re_o than large Re_o.

Calculations for XM687 shell spin decay were compared with yawsonde measurements for 100% and 90%-filled cases. The 100%-filled cases show excellent agreement between the theory and the measurement throughout the entire flight, the errors being less than 0.8% of the measured spin rate. Spin decay for 90%-filled cases are not quite as accurately described by the present theory, but the errors are no larger than about 1%. The largest errors occur in the 90%-filled case at high Reynolds number where the boundary layers are expected to be turbulent over part of the endwall.

The spin records discussed in this report all exhibit smooth spin decay throughout the flight. There are other types of spin records that cannot be predicted by the present theory. When the XM687 shell is launched with large yaw the spin history can be quite different from that shown in Figures 5 - 8. In these cases the spin history is characterized by a much more rapid initial spin decay, which is almost linear for approximately one to two seconds, followed by a sharp change to a smaller rate of decay. This spin record with a "corner" is not predicted by the methods described in this report. A method for treating the spin decay in such cases is discussed in Reference 3.

Calculations with Method I have been used to determine the spin-up time, t_s; defined as the time when 99% of the instantaneous rigid-body angular momentum is achieved. For the XM687 considered here, t_s varies from 0.9s for $Re_o = 3320$ to about 19s for $Re_o \sim 1\times10^6$. These predictions for t_s are based on Wedemeyer's spin-up model which is valid for small yaw. When the projectile yaw is large, the toroidal vortex model discussed in Reference 3 may be more appropriate for determining a measure of the spin-up time.

VII. ACKNOWLEDGEMENT

Miss J. M. Bartos developed computer programs used for the numerical calculations with Method II. The authors are grateful to Drs. W. P. D'Amico, Jr., A. Mark and R. Sedney for discussions and advice during the course of this work.

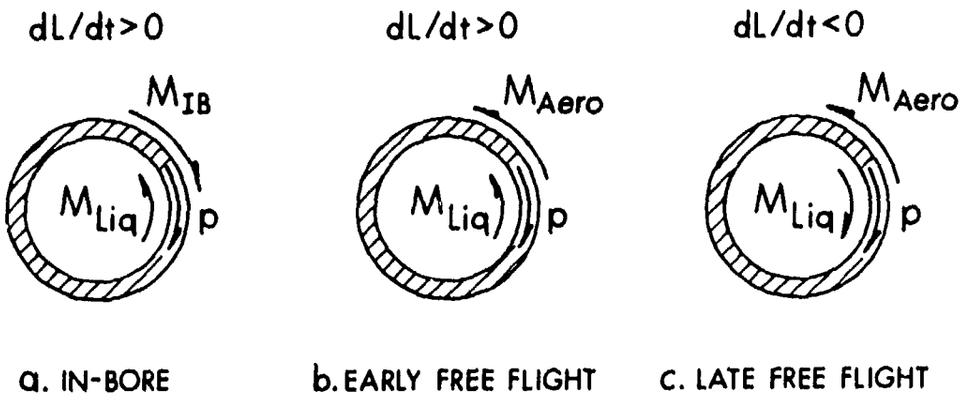

Figure 1. Moments Acting on a Spinning Liquid-Filled Projectile; A Free-Body Diagram of Casing During Launch and Free Flight

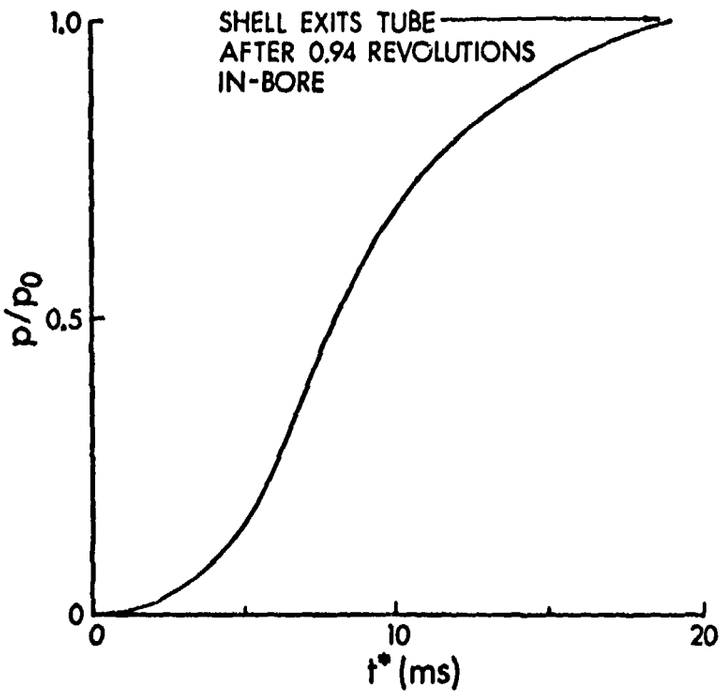

Figure 2. Normalized In-Bore Spin History for a Typical XM687 Shell (Round 7670) Launched from the M109 Howitzer at Charge 3, p_0 = 92.3 rev/s

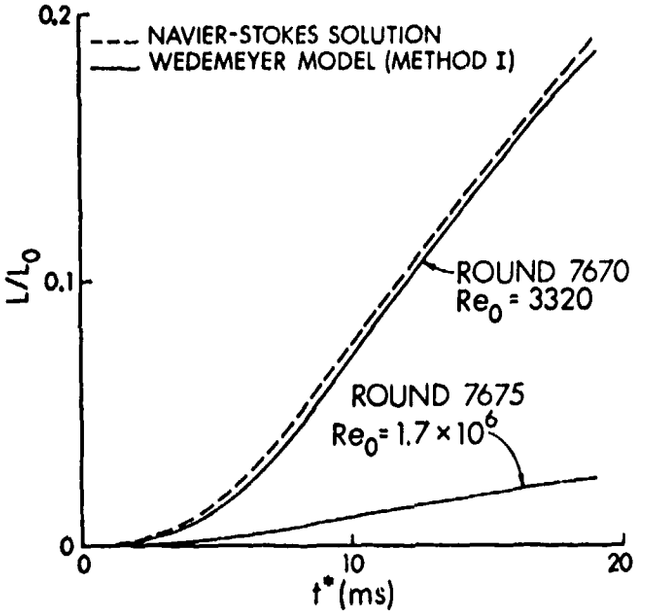

Figure 3. Normalized In-Bore Liquid Angular Momentum History for Two XM687 Shell with Different Launch Reynolds Numbers

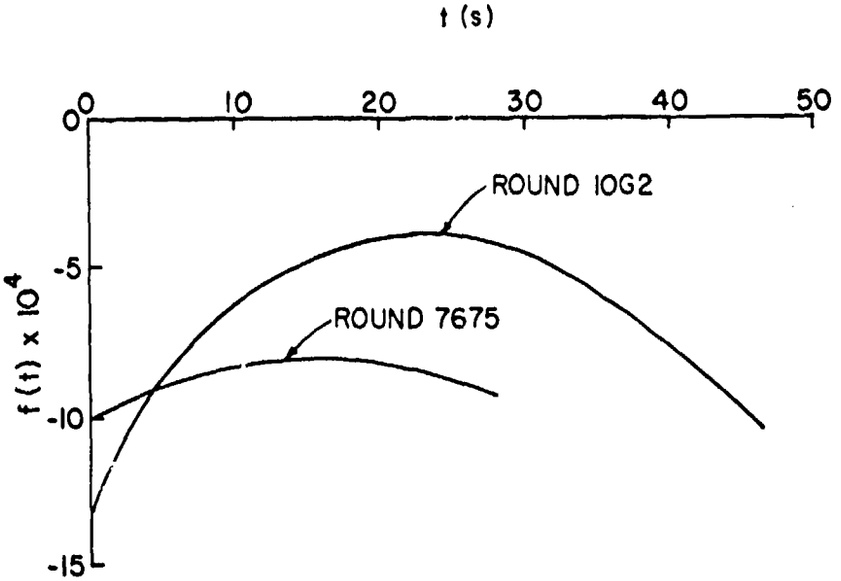

Figure 4. Spin Damping Function f(t) for Two Representative XM687 Shell

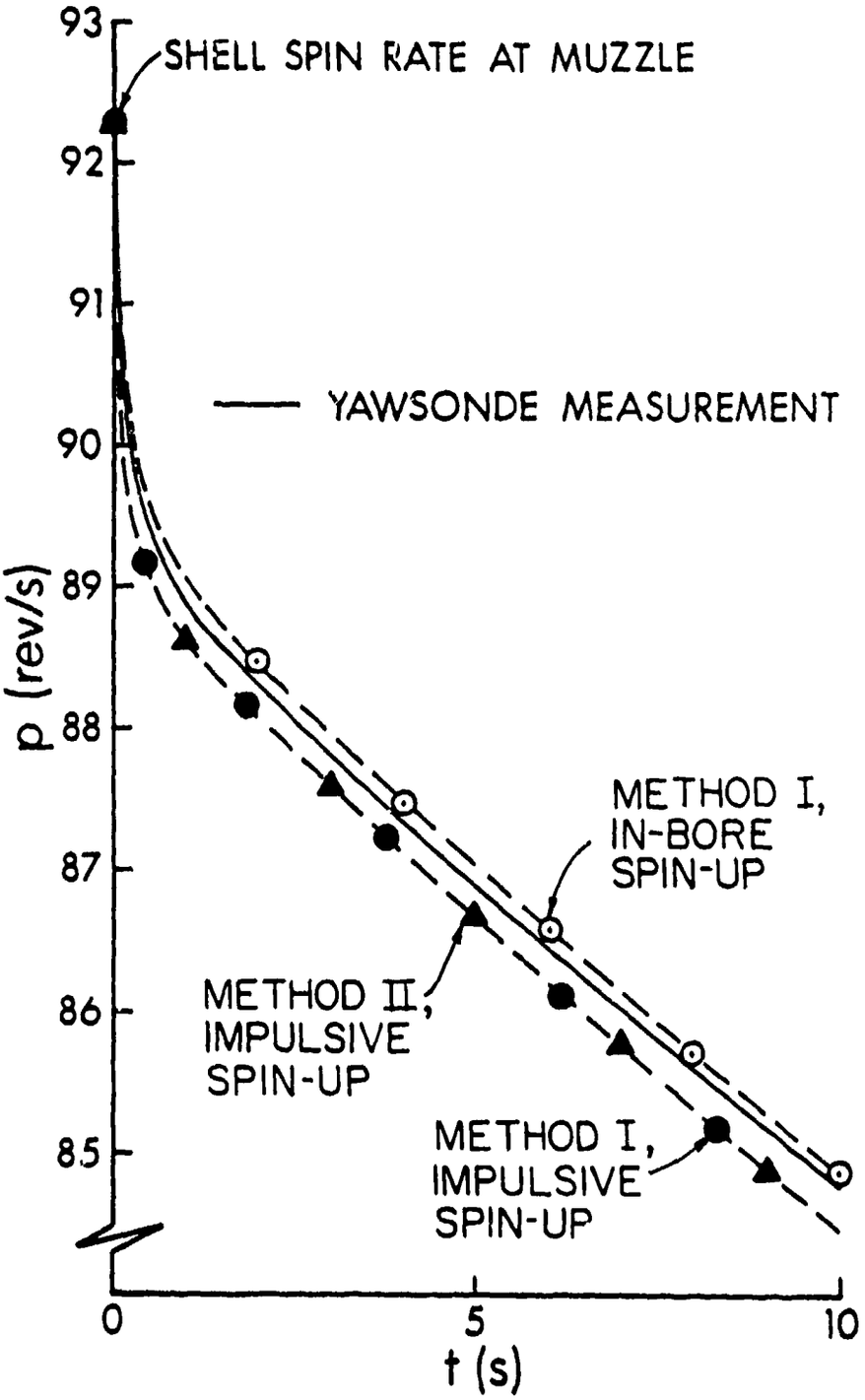

Figure 5. Shell Spin Decay for 100%-Filled Round 7670 with Re_o = 3320 and Laminar Endwall Boundary Layer

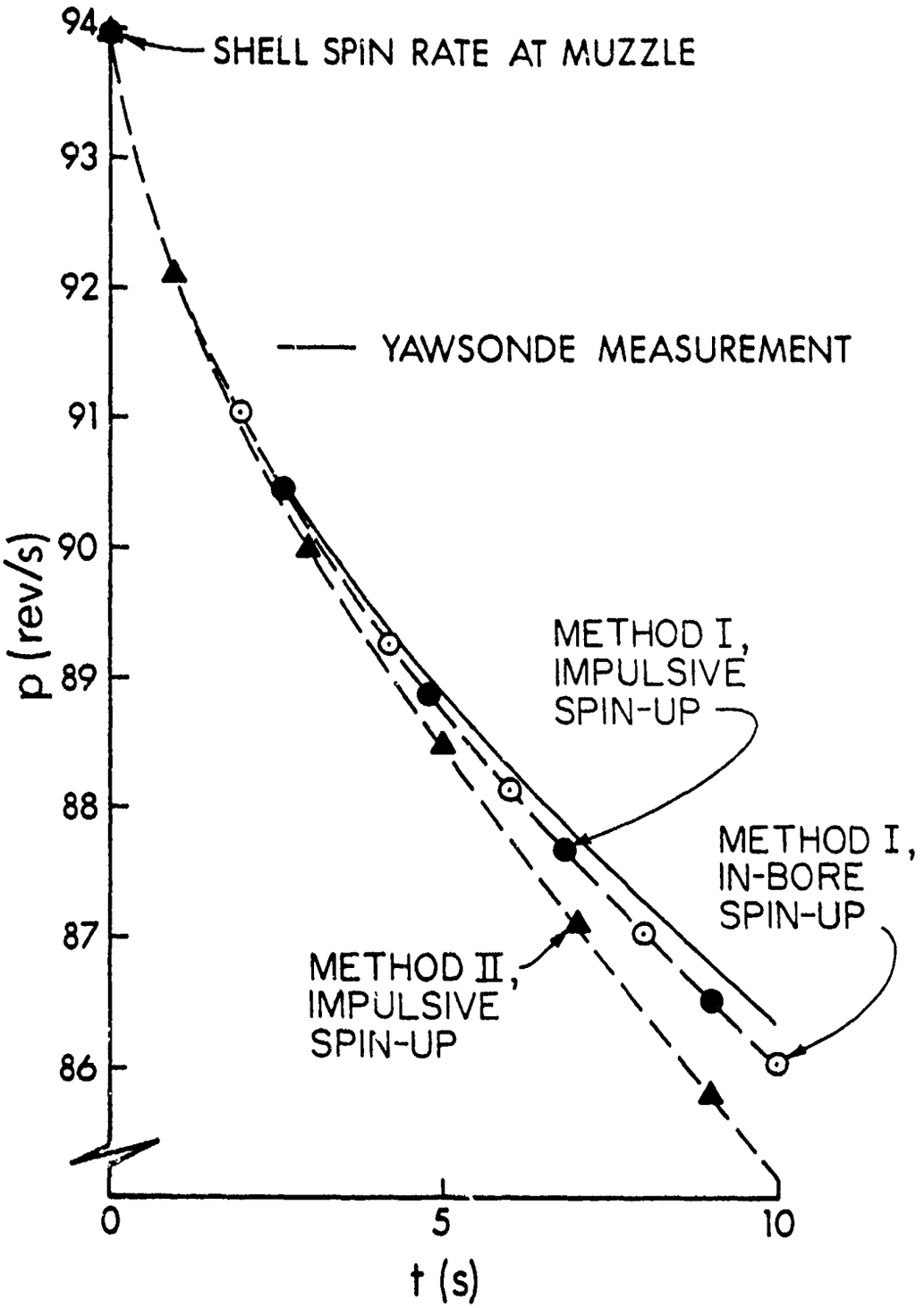

Figure 6. Shell Spin Decay for 100%-Filled Round 7675 with $Re_o = 1.7 \times 10^6$ and Turbulent Endwall Boundary Layer

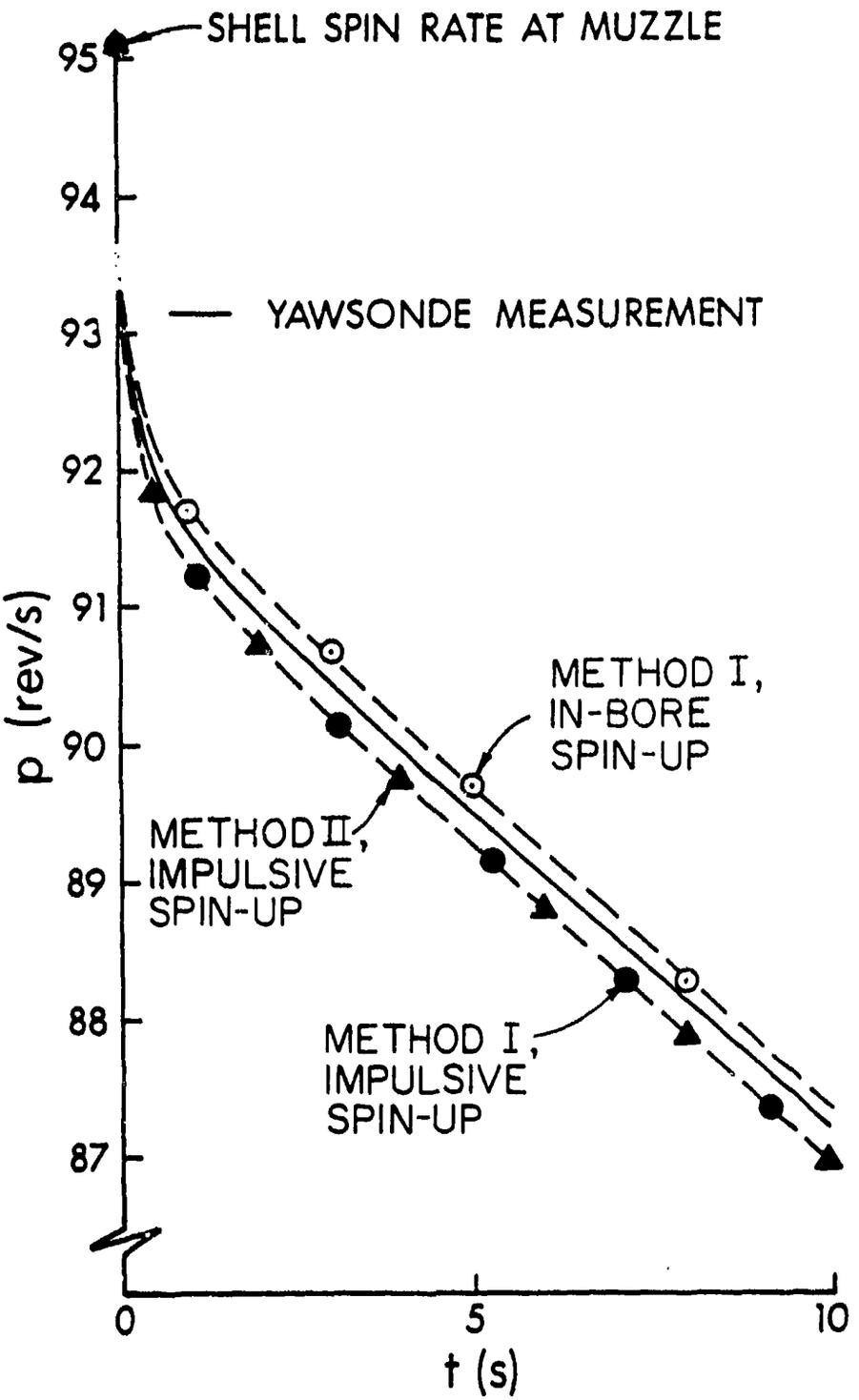

Figure 7. Shell Spin Decay for 90%-Filled Round 7677 with Re_0 = 3421 and Laminar Endwall Boundary Layer

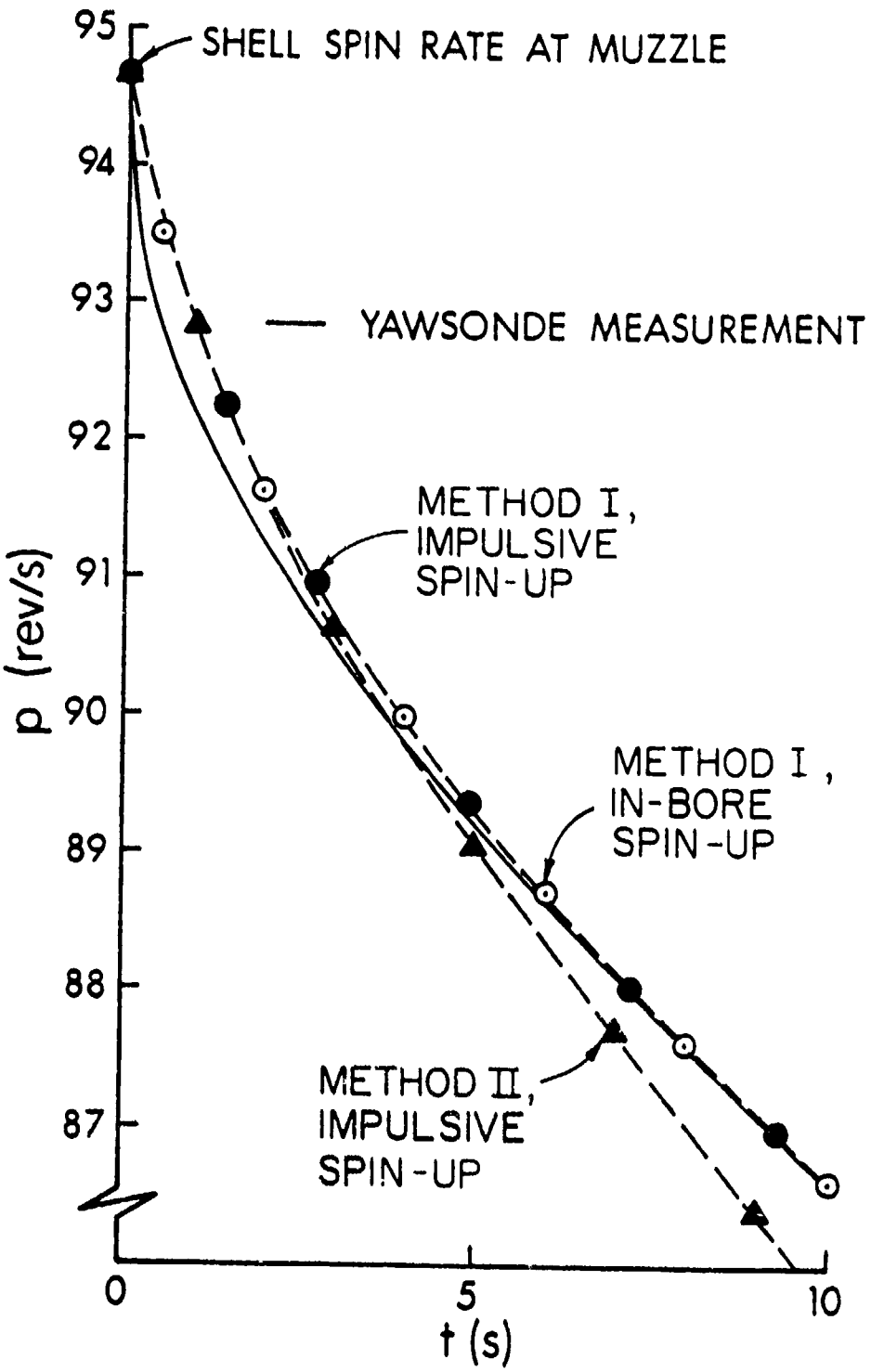

Figure 8. Shell Spin Decay for 90%-Filled Round 7676 with $Re_0 = 1.7 \times 10^6$ and Turbulent Endwall Boundary Layer

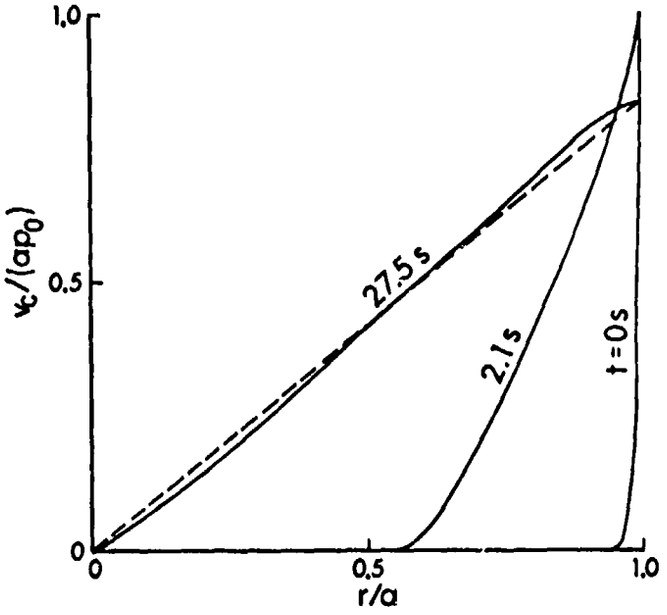

Figure 9. Azimuthal Velocity Profiles for Round 7675 with $Re_0 = 1.7\times10^6$ and Turbulent Endwall Boundary Layer

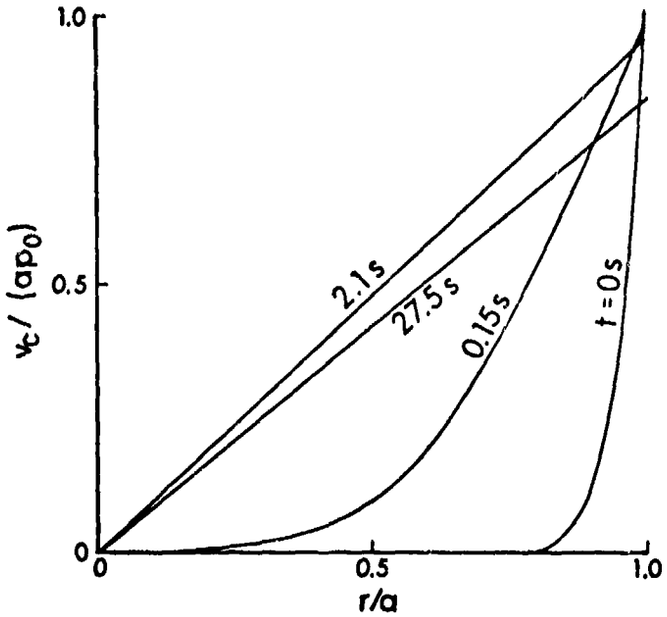

Figure 10. Azimuthal Velocity Profiles for Round 7670 with $Re_0 = 3320$ and Laminar Endwall Boundary Layer

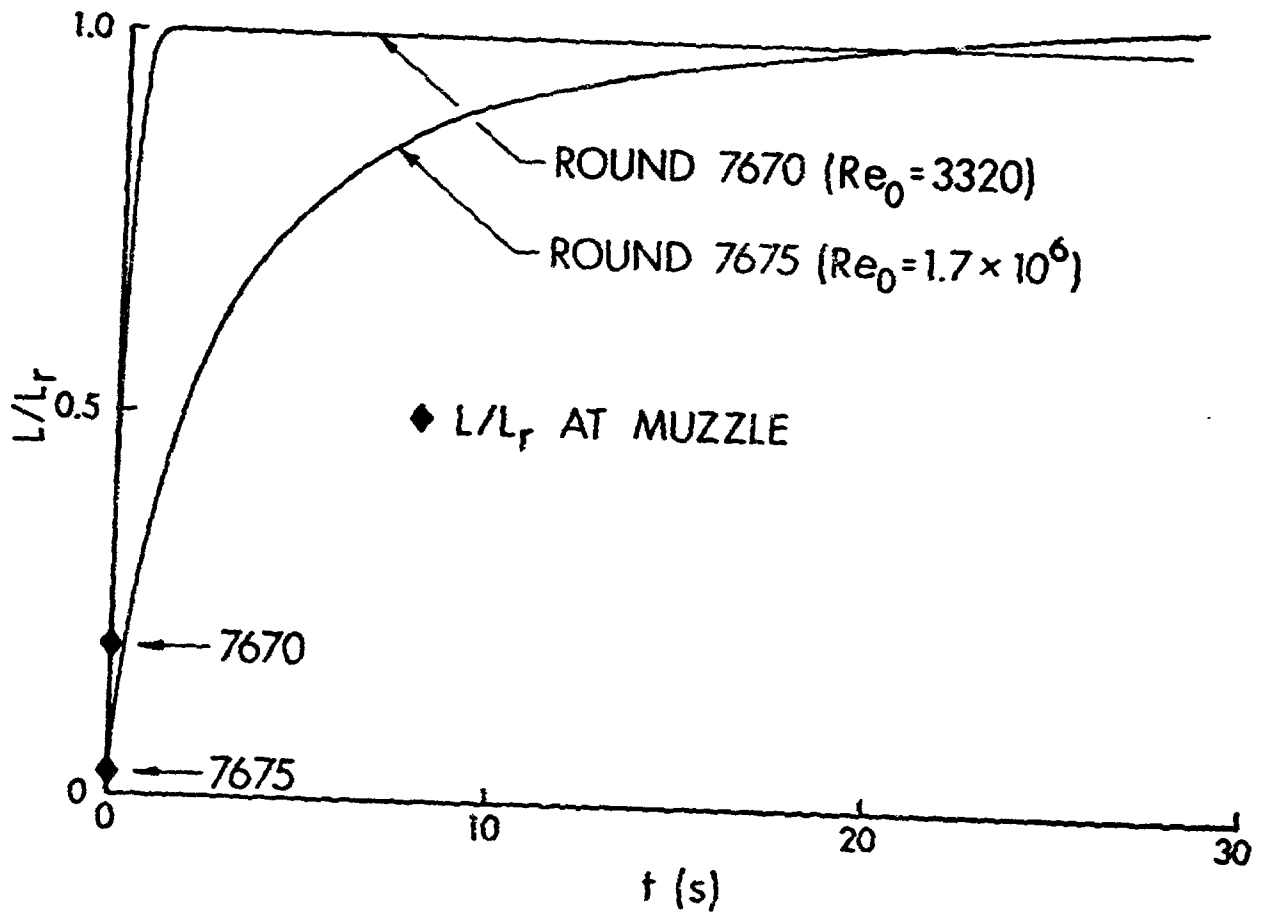

Figure 11. Angular Momentum History for Liquid Predicted by Method I

REFERENCES

1. E. H. Wedemeyer, "The Unsteady Flow Within a Spinning Cylinder," J. Fluid Mech., Vol. 20, Part 3, 1964, pp. 383-399. Also see BRL Report 1252, Aberdeen Proving Ground, MD, October 1963. (AD 431846)

2. A. Mark and W. H. Mermagen, "Measurement of Spin Decay and Instability of Liquid-Filled Projectiles Via Telemetry," BRL Memorandum Report 2333, Aberdeen Proving Ground, MD, October 1973. (AD 771919)

3. C. W. Kitchens, Jr., and R. Sedney, "Conjecture for Anomalous Spin Decay of the 155mm Binary Shell (XM687)," BRL Memorandum Report (in preparation).

4. R. Sedney and N. Gerber, "Viscous Effects in the Wedemeyer Model of Spin-Up from Rest," BRL Report (in preparation).

5. B. G. Karpov, "Dynamics of Liquid-Filled Shell: Instability During Spin-Up," BRL Memorandum Report 1269, Aberdeen Proving Ground, MD, January 1965. (AD 463926)

6. S. G. Rubin and T. C. Lin, "A Numerical Method for Three-Dimensional Viscous Flow: Application to the Hypersonic Leading Edge," J. Comp. Phys., Vol. 9, 1972, pp. 339-364.

7. C. W. Kitchens, Jr., "Navier-Stokes Solutions for Spin-Up from Rest in a Cylindrical Container," BRL Report (in preparation).

8. A. Mark, "Measurement of Angular Momentum Transfer in Liquid-Filled Shell," BRL Report (in preparation).

9. V. Oskay and J. H. Whiteside, "Flight Behavior of 155mm (XM687 Mod I and XM687 Mod II) and 8-Inch (XM736 Mod I) Binary Shell at Nicolet, Canada, During the Winter of 1974-1975," BRL Memorandum Report 2608, Aberdeen Proving Ground, MD, March 1976. (AD B010566L)

10. Engineering Design Handbook, Liquid-Filled Projectile Design, AMC Pamphlet No. 706-165, U.S. Army Materiel Command, Washington, DC, April 1969, p. 8-4. (AD 853719)

LIST OF SYMBOLS

a	radius of shell cylindrical cavity (= 0.0535 m for non-standard XM687 cavity)
c	half-height of cylindrical cavity (= 0.237 m for non-standard XM687 cavity)
$f(t)$	defined by Eq. (13) ($kg\text{-}m^2/s$)
ℓ	projectile diameter (= 0.1524 m for XM687 shell)
p	instantaneous spin rate of shell (s^{-1})
p_o	shell spin rate at muzzle (s^{-1})
r	radial coordinate (m)
t	time measured from instant of projectile release from gun tube (s)
t^*	time measured from the beginning of projectile in-bore motion (s)
t_s	time at which the fluid angular momentum reaches 99% of the rigid-body angular momentum based on p_o (s)
u_c	radial velocity component in core flow in Wedemeyer spin-up model (m/s)
v	azimuthal velocity component in liquid (m/s)
v_c	azimuthal velocity component in core flow in Wedemeyer spin-up model (m/s)
w_c	axial velocity component in core flow in Wedemeyer spin-up model (m/s)
z	axial coordinate measured from cavity rear endwall (m)
C_{ℓ_p}	projectile roll damping coefficient (nondimensional)
I_z	axial moment of inertia of projectile casing ($kg\text{-}m^2$)
L	liquid angular momentum ($kg\text{-}m^2/s$)
L_o	rigid-body angular momentum of liquid at spin rate p_o ($kg\text{-}m^2/s$)
L_r	rigid-body angular momentum of liquid at spin rate p ($kg\text{-}m^2/s$)

LIST OF SYMBOLS (continued)

M_{IB}	in-bore moment acting on shell due to gun tube twist (N-m)
M_{Aero}	aerodynamic moment acting on shell due to air shear (N-m)
M_{Liq}	liquid moment acting on shell due to shear stress at cavity walls (N-m)
P_c	pressure (N/m^2)
Re	Reynolds number of shell defined by Eq. (9) (nondimensional)
Re_o	launch Reynolds number of shell defined by Eq. (14) (nondimensional)
S	maximum cross-sectional area of the projectile (= 0.01824 m^2 for XM687 shell)
V_o	muzzle-velocity of projectile (m/s)
V	instantaneous projectile velocity (m/s)
β	fill ratio of cylinder; fluid volume divided by total cavity volume (nondimensional)
ε	tolerance on angular momentum convergence from iteration to iteration
θ	angular coordinate
ν	kinematic viscosity of liquid (m^2/s)
ρ	liquid payload density (kg/m^3)
ρ_a	air density (kg/m^3)
ω	local liquid angular velocity (= v/r) (s^{-1})
ω_c	local liquid angular velocity in core (= v_c/r) (s^{-1})

Superscript

i	iteration level i

Subscript

n	time level n

DISTRIBUTION LIST

No. of Copies	Organization
12	Commander Defense Documentation Center ATTN: DDC-TCA Cameron Station Alexandria, VA 22314
1	Commander US Army Materiel Development and Readiness Command ATTN: DRCDMA-ST 5001 Eisenhower Avenue Alexandria, VA 22333
1	Commander US Army Aviation Systems Command ATTN: DRSAV-E 12th and Spruce Streets St. Louis, MO 63166
2	Commander US Army Air Mobility Research and Development Laboratory ATTN: SAVDL-D W. J. McCroskey Ames Research Center Moffett Field, CA 94035
1	Commander US Army Electronics Command ATTN: DRSEL-RD Fort Monmouth, NJ 07703
1	Commander US Army Jefferson Proving Gd ATTN: STEJP-TD-D Madison, IN 47250
3	Commander US Army Missile Research & Development Command ATTN: DRDMI-TD Ray Deep DRDMI-R Redstone Arsenal, AL 35809
1	Commander US Army Tank Automotive Development Command ATTN: DRDTA-RWL Warren, MI 48090
2	Commander US Army Mobility Equipment Research & Development Com. ATTN: Tech Docu Cen, Bldg 315 DRSME-RZT Fort Belvoir, VA 22060
1	Commander US Army Armament Materiel Readiness Command Rock Island, IL 61202
1	Commander US Army Armament Research & Development Command ATTN: DRDAR-LCA-F, A. Loeb Dover, NJ 07801
1	Commander US Army Harry Diamond Labs ATTN: DRXDO-TI 2800 Powder Mill Road Adelphia, MD 20783
1	Director US Army TRADOC Systems Analysis Activity ATTN: ATAA-SA White Sands Missile Range NM 88002
1	Commander US Army Research Office ATTN: R. E. Singleton P. O. Box 12211 Research Triangle Park NC 27709

DISTRIBUTION LIST

No. of Copies	Organization
1	Commander US Army Waterways Experiment Station ATTN: R. H. Malter Vicksburg, MS 39180
1	AGARD-NATO ATTN: R. H. Korkegi APO New York 09777
3	Commander US Naval Air Systems Command ATTN: AIR-604 Washington, DC 20360
3	Commander US Naval Ordnance Systems Command ATTN: ORD-0632 ORD-035 ORD-5524 Washington, DC 20360
2	Commander David W. Taylor Naval Ship Research & Development Command ATTN: H. J. Lugt, Code 1802 S. de los Santos Head, High Speed Aero Div Bethesda, MD 20084
6	Commander US Naval Surface Weapons Center Applied Aerodynamics Division ATTN: K. R. Enkenhus M. Ciment K. Lobb S. M. Hastings A. E. Winklemann W. C. Ragsdale Silver Spring, MD 20910
1	Commander US Naval Surface Weapons Ctr ATTN: Tech Library Dahlgren, VA 22448
1	AFATL (DLDL, Dr. D.C. Daniel) Eglin AFB, FL 32542
2	AFFDL (W.L. Hankey; J.S. Shang) Wright-Patterson AFB, OH 45433
7	Director National Aeronautics and Space Administration ATTN: F. R. Bailey D. R. Chapman J. Marvin J. D. Murphy J. Rakich W. C. Rose B. Wick Ames Research Center Moffett Field, CA 94035
6	Director National Aeronautics and Space Administration Langley Research Center ATTN: J. E. Carter J. E. Harris E. Price J. South J. R. Sterrett Tech Lib Langley Station Hampton, VA 23365
1	Director National Aeronautics and Space Administration Lewis Research Center ATTN: MS 60-3, Tech Lib 21000 Brookpark Road Cleveland, OH 44135

DISTRIBUTION LIST

No. of Copies	Organization
1	Director National Aeronautics and Space Administration Marshall Space Flight Center ATTN: A. R. Felix, Chief S&E-AERO-AE Huntsville, Al 35812
2	Director Jet Propulsion Laboratory ATTN: J. Kendall Tech Lib 4800 Oak Grove Drive Pasadena, CA 91103
3	ARO, Inc. ATTN: J. D. Whitfield R. K. Matthews J. C. Adams Arnold AFB, TN 37389
3	Aerospace Corporation ATTN: T. D. Taylor H. Mirels R. L. Varwig Aerophysics Lab P. O. Box 92957 Los Angeles, CA 90009
1	AVCO Systems Division ATTN: B. Reeves 201 Lowell Street Wilmington, MA 01887
3	The Boeing Company Commercial Airplane Group ATTN: W. A. Bissell, Jr. M. S. 1W-82, Org 6-8340 P. E. Rubbert J. D. McLean Seattle, WA 98124
2	Calspan Corporation ATTN: A. Ritter M. S. Holden P. O. Box 235 Buffalo, NY 14221
1	Center for Interdisciplinary Programs ATTN: Victor Zakkay W. 177th St. & Harlem River Bronx, NY 10453
1	General Dynamics ATTN: Research Lib 2246 P. O. Box 748 Fort Worth, TX 76101
1	General Electric Company ATTN: H. T. Nagamatsu Research & Development Lab (Comb. Bldg.) Schenectady, NY 12301
1	General Electric Co., RESD ATTN: R. A. Larmour 3198 Chestnut Street Philadelphia, PA 19101
3	Grumman Aerospace Corporation ATTN: R. E. Melnik L. G. Kaufman B. Grossman Research Department Bethpage, NY 11714
2	Lockheed-Georgia Company ATTN: B. H. Little, Jr. G. A. Pounds Dept 72074, Zone 403 86 South Cobb Drive Marietta, GA 30062

DISTRIBUTION LIST

No. of Copies	Organization
1	Lockheed Missiles & Space Co. ATTN: Tech Info Center 3251 Hanover Street Palo Alto, CA 94304
4	Martin-Marietta Laboratories ATTN: S. H. Maslen S. C. Traugott K. C. Wang H. Obremski 1450 S. Rolling Road Baltimore, MD 21227
2	McDonnell Douglas Astronautics Corporation ATTN: J. Xerikos H. Tang 5301 Bolsa Avenue Huntington Beach, CA 92647
1	McDonnell-Douglas Corporation Douglas Aircraft Company ATTN: T. Cebeci 3855 Lakewood Boulevard Long Beach, CA 90801
1	Northrup Corporation Aircraft Division ATTN: S. Powers 3901 W. Broadway Hawthorne, CA 90250
2	Sandia Laboratories ATTN: F. G. Blottner Tech Lab P. O. Box 5800 Albuquerque, NM 87115
2	United Aircraft Corporation Research Laboratories ATTN: R. W. Briley Library East Hartford, CT 06108
1	Vought Systems Division LTV Aerospace Corporation ATTN: J. M. Cooksey Chief, Gas Dynamics Lab., 2-53700 P. O. Box 5907 Dallas, TX 75222
1	California Institute of Technology Guggenheim Aeronautical Lab ATTN: Tech Lib Pasadena, CA 91104
2	California Institute of Technology ATTN: H. B. Keller Mathematics Dept. D. Coles Aeronautics Dept. Pasadena, CA 91109
1	Cornell University Graduate School of Aero Engr ATTN: Library Ithaca, NY 14850
2	Illinois Institute of Tech ATTN: M. V. Morkovin H. M. Nagib 3300 South Federal Chicago, IL 60616
1	The Johns Hopkins University ATTN: S. H. Davis Dept of Mechanics and Materials Science Baltimore, MD 21218
1	Louisiana State University Department of Physics ATTN: R. G. Hussey Baton Rouge, LA 70803

DISTRIBUTION LIST

No. of Copies	Organization
2	Massachusetts Institute of Technology ATTN: E. Covert Tech. Library 77 Massachusetts Avenue Cambridge, MA 02139
2	North Carolina State University Mechanical and Aerospace Engineering Department ATTN: F. F. DeJarnette J. C. Williams Raleigh, NC 27607
1	Notre Dame University ATTN: T. J. Mueller Dept. of Aero Engr South Bend, IN 46556
2	Ohio State University Dept. of Aeronautical and Astronautical Engineering ATTN: S. L. Petrie O. R. Burggraf Columbus, OH 43210
2	Polytechnic Institute of New York ATTN: G. Moretti S. G. Rubin Route 110 Farmingdale, NY 11735
1	Princeton University Dept. of Aerospace and Mechanical Sciences ATTN: S. I. Cheng Princeton, NJ 08540
3	Princeton University James Forrestal Research Center Gas Dynamics Laboratory ATTN: I. E. Vas S. M. Bogdonoff Tech Lib Princeton, NJ 08540
1	Purdue University Thermal Science & Prop Center ATTN: D. E. Abbott W. Lafayette, IN 47907
1	Rensselaer Polytechnic Institute Dept. of Math. Sciences ATTN: R. C. DiPrima Troy, NY 12181
1	Rutgers University Dept. of Mechanical, Industrial and Aerospace Engineering ATTN: R. H. Page New Brunswick, NJ 08903
1	Southern Methodist University Dept. of Civil & Mechanical Engineering ATTN: R. L. Simpson Dallas, TX 75275
1	Southwest Research Institute Applied Mechanics Reviews 8500 Culebra Road San Antonio, TX 78228
1	University of California - Berkley Dept. of Aerospace Engineering ATTN: M. Holt Berkeley, CA 94720
1	University of California - Davis ATTN: H. A. Dwyer Davis, CA 95616
2	University of California - San Diego Dept. of Aerospace Engineering & Mechanical Engr Sciences ATTN: P. Libby Tech Lib La Jolla, CA 92037

DISTRIBUTION LIST

No. of Copies	Organization
2	University of Cincinnati Dept. of Aerospace Engineering ATTN: R. T. Davis M. J. Werle Cincinnati, OH 45221
1	University of Colorado Dept. of Astro-Geophysics ATTN: E. R. Benton Boulder, CO 80302
1	University of Hawaii Dept. of Ocean Engineering ATTN: G. Venezian Honolulu, HI 96822
2	University of Maryland ATTN: W. Melnik J. D. Anderson College Park, MD 20740
1	University of Michigan Department of Aeronautical Engineering ATTN: Tech Lib East Engineering Building Ann Arbor, MI 48104
1	University of Santa Clara Department of Physics ATTN: R. Greeley Santa Clara, CA 95053
3	University of Southern Cal. Dept. of Aerospace Engineering ATTN: T. Maxworthy P. Weidman M. Hafez Los Angeles, CA 90007
1	University of Texas Dept of Aerospace Engineering ATTN: J. C. Westkaemper Austin, TX 78712
1	University of Virginia Dept. of Aerospace Engineering & Engineering Physics ATTN: I. D. Jacobson Charlottesville, VA 22904
1	University of Washington Dept. of Mechanical Engineering ATTN: Tech Lib Seattle, WA 98195
2	Virginia Polytechnic Institute Dept. of Aerospace Engineering ATTN: G. R. Inger F. J. Pierce Blacksburg, VA 24061

Aberdeen Proving Ground

Marine Corps Ln Ofc
Dir, USAMSAA

Munitions Systems Division
Bldg. 3330
ATTN: E. A. Jeffers
W. C. Dee
W. J. Pribyl
APG-EA

Armament Concepts Office
Bldg. 3516 (DRDAR-ACW)
ATTN: M. C. Miller
APG-EA